Studying Mountain Glacier Processes Using a Staring Instrument

Andrea Donnellan, Bruce Bills, Joseph J. Green,
Renaud Goullioud, Susan Jones, Russell Knight,
Michael Underhill, Jay Goguen,
Eric M. De Jong, Adnan Ansar
Jet Propulsion Laboratory
California Institute of Technology
4800 Oak Grove Dr.
Pasadena, CA 91109
818-354-4737
[Andrea.Donnellan] [Bruce.Bills] [Joseph.J.Green]
[Renaud.Goullioud] [Susan.K.Jones] [Russell.L.Knight]
[Michael.L.Underhill] [Jay.Goguen] [Eric.M.DeJong]
[Adnan.Ansar]@jpl.nasa.gov

Ted Scambos
National Snow and Ice Data Center
University of Colorado
Boulder, CO 80309-0449
303-492-1113
teds@nsidc.org

Paul Morin
Polar Geoscience Center
University of Minnesota
Saint Paul, MN 55108
612-625-6090
lpaul@umn.edu

Bernard Hallet
Quaternary Research Center
University of Washington
Seattle, WA 98195
206-685-2409
hallet@u.washington.edu

Lonnie Thompson
Byrd Polar Research Center
Ohio State University
Columbus, OH 43210
614-292-6652
thompson.3@osu.edu

Alex S. Gardner
Graduate School of Geography
Clark University
950 Main Street
Worcester, MA 01610-1477
508-793-7325
agardner@clarku.edu

Jared Ekholm
Air Force Research Laboratory
Rome, NY
jared.ekholm@us.af.mil

Abstract— Mountain glaciers around the globe are retreating rapidly, but the exact mechanisms causing the retreat are not well understood. Is warming of the atmosphere the key driver? What are the roles of changes in surface albedo due to contaminants and snow optical grain size and surface roughness? Improved understanding of the response of mountain glaciers to global and environmental change is key to answering these questions. A staring instrument that provides measurements from multiple viewing and illumination angles enables simultaneous measurement of 3D surface structure, including texture, material characteristics, and albedo. Such measurements make it possible to determine melt due to absorbed solar energy separately from melt due to other sources. The International Space Station (ISS) provides a possible host platform for a staring instrument that could access all tropical and most temperate mountain glaciers. The non-sun-synchronous orbit enables varying solar illumination angles.

TABLE OF CONTENTS

1. INTRODUCTION

Mountain glaciers and polar ice caps are losing mass to the world's oceans at an accelerated rate, accounting for $29 \pm 13\%$ of all sea level rise between 2003 and 2009 [1]. Mountain glaciers are particularly sensitive to global environmental change [e.g., 2] because much of their surface is at or near the melting point; any additional energy input contributes directly to melt. Low-latitude glaciers and seasonal snow feed the headwaters of streams and rivers that provide drinking water, irrigation, and hydropower for over one billion people [3]. Conversely, glaciers can pose flood and avalanche hazards in some areas.

Mission to Understand Ice Retreat (MUIR) is a staring instrument concept to determine the relative contributions of global and environmental change to the response of mountain glaciers. We discuss here the technology, science, and a point design for a payload hosted on the International Space Station (ISS). In this paper we do not examine other designs that may also meet the requirements.

The delicate balance between accumulation and ablation determines the health of a glacier. A glacier that receives more mass from snow than it sheds through melt water runoff and calving will grow (positive mass budget) and a glacier that loses more than it gains will shrink (negative mass budget). Absorption of solar radiation is typically the largest energy source contributing to melt, but it varies greatly in space and time. Solar absorption over a glacier surface can vary by a factor of 6-7 due solely to differences in albedo; fresh snow absorbs about 10% of incident solar radiation whereas dirty ice absorbs 60-80%. Snow albedo is highly sensitive to small amounts of impurities (black carbon, dust and ash), and albedo exerts a major control on the surface energy balance [4]. Quantifying the glacier surface albedo and impurity concentration, and tracking changes in albedo over the annual cycle, is necessary to understand glacier response to changes in cloudiness, snow input, or expected changes in impurities over time. Systematic study of the evolution of glacier surfaces and the processes influencing their albedo for hundreds of mountain glaciers would represent a tremendous advance in understanding global glacier loss and the likely impacts of future climate change on these sensitive systems.

Global climate change and glacier surface contamination from dust and soot have both been implicated in the rapid retreat of glaciers. However, partitioning of the impacts between the two is not well understood, and the manifestations of the impacts of warmer air or changes in net snow accumulation from global climate change are uncertain. Simultaneously measuring glacier volume changes, flow speed changes, albedo changes, and details of surface structure can provide a means assessing the components of the mass balance (input versus melt) and the dynamical processes of a glacier system.

Albedo depends on the spectral frequency of the radiation, and the directional distribution of reflected radiation. Achieving the best estimate of albedo of a glacier surface requires measurement of directional surface reflectance to accurately characterize surface scattering. This requires measurements from many different viewing and illumination angles.

Surface structural characteristics are informative of glacier processes, which can include melt, wind and sublimation, or sparse debris cover. These can be derived from surface texture and response at different spectral bands. Wind-formed micro-relief features on snow may be ablation-related or accumulation-related (e.g., dunes) and are dependent on particle supply, humidity, temperature, and wind regime [5]; understanding their structure is informative of transport [6]. Ice type, age, maturity, contamination, and water distribution can be inferred from spectral bands and texture. Surface structures can also include sun cups or ablationary snow pinnacles called penitentes. Texture is best determined from variable viewing and illumination angles (and post-processing), and other surface properties can be inferred from multispectral bands.
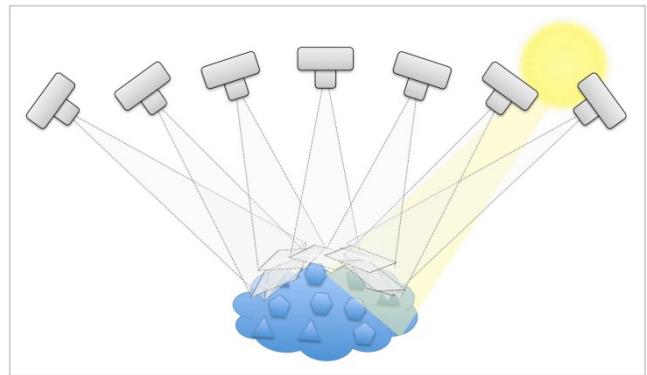

Figure 1. A staring instrument tracks and stares at a target over a range of vantage points during a pass. From a non-sun-synchronous orbit, data acquisitions occur with a variety of solar illuminations.

2. STARING IMAGING

Staring imaging is the acquisition of multiple or continuous data while observing a fixed target point. From a moving platform, staring imaging observes the target from a variety of perspectives during a single pass. Different passes would occur under different lighting conditions for staring imagers in non-sun-synchronous orbits. The range of viewing and illumination geometries of a spaceborne staring instrument makes it unique for producing surface topography, extracting reflectance and albedo, and for observing rapid and episodic events. Staring at a target offers the ability to probe its characteristics, allowing retrieval of 3D structure, bidirectional reflectance, and their changes on fine and coarse scales. It also allows rapidly changing features to be tracked over short time scales because a stare could last several minutes depending on the orbit. Such features could include icebergs of different sizes drifting at varying rates and responding to currents from different parts of the water column near a large number of calving glaciers that display diverse and poorly understood volume changes in part due to submarine melting. Features could be cataloged over many orbit passes in order to build up detailed understanding of their characteristics and changes over time.

Staring imaging provides the ability to characterize coarse and fine-scale surface structure and changes over time, providing information about processes and forcings. Appearance of a surface depends on lighting and viewing directions. Surface textures exhibit complex reflectance properties that include shadowing and multiple reflections amongst facets [7]. The Bidirectional Reflectance Distribution Function (BRDF) represents course scale features and the Bidirectional Texture Function (BTF) represents fine scale variations that give rise to local intensity variations [8]. Spaceborne measurements of surface characteristics are typically made for one view during a pass, or for the Multi-angle Imaging Spectro-Radiometer (MISR) up to 9 fixed views. To maximize the Signal to Noise Ratio (SNR) the spacecraft are in high sun elevation sun-synchronous orbits resulting in one illumination angle.
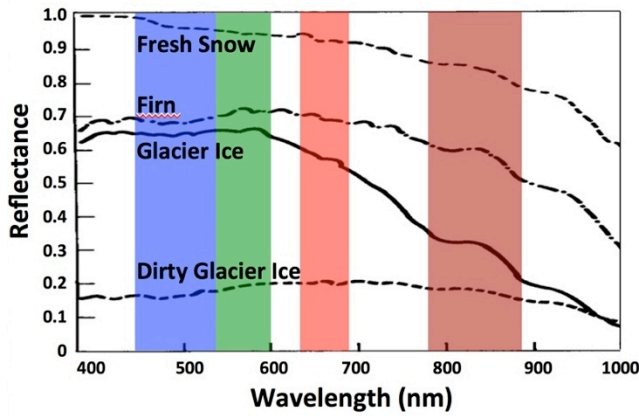
Figure 2. Reflectance spectra for different snow and ice surfaces [9] with recommended MUIR bands.

Improved measurements of glacier surfaces demand multi-angle and multispectral measurements over a diverse range of solar and observing elevation angles. The concern here is to focus on select targets to recover detailed changing surface properties. This can be best accomplished with a staring system in low Earth orbit (LEO). By staring, we mean that the telescope is continuously pointing to the same surface location while imaging it with a 2D Focal Plane Array (FPA). By canceling out the principal viewing geometry dynamics, the system design space is freed to enable high resolution imaging without the restriction on integration time to achieve a high SNR. What remains of the viewing geometry dynamic enhances the science objectives. As the system flies over the target, the perspective smoothly changes, permitting multi-angle measurements for understanding topography on broad and fine scales (Figure 1). With longer integration times possible with a FPA, non-sun-synchronous orbits can be employed to yield target illumination diversity for a detailed understanding of surface properties.

Staring imaging complements imagery collected from push-broom systems such as Worldview-2 and ASTER. These broad area mappers produce Digital elevation models (DEMs), geometry, and surface features of ice masses. Push-broom systems are primarily optimized for broad area mapping applications with area-rate-coverage being a dominant concern. Traditional remote sensing platforms in Low-Earth-Orbit (LEO) employ linear arrays to image in one-axis as the instrument sweeps over an area of interest to fill in the second dimension. This push-broom modality requires these systems to achieve a high SNR in very short-integration times confining them to operate in sun-synchronous orbits with highly under-sampled spectral bands in their imagers.

Staring imaging acquires a set of images per filter of a glacier over a large range of viewing angles during a pass. Filters would be optimized to discriminate different types of glacier surface ice types (Figure 2). Surface topography DEMs can be constructed using 'structure from motion' methods [10, 11]. The DEM defines the local incidence and emission angle of resolved facets and facet intensity measures the bidirectional reflectance distribution function (BRDF), which can be integrated for albedo. Multispectral measurements should cover the spectral region where ice has the highest albedo and the strongest impact on the absorbed solar energy.

A simple ice pinnacle (or penitentes) model demonstrates that a rough surface causes a strong emission and incidence angle dependence of the reflectance (Figure 3). Reflectance varies considerably for rough surfaces for different viewing and illumination angles. From a single viewing geometry, it is difficult to tell flat dark surfaces from rough white surfaces. Staring capability is particularly well suited for separating glacier surface texture variations from albedo variations. The variation of reflectance with illumination and viewing geometry makes features such as ice and snow
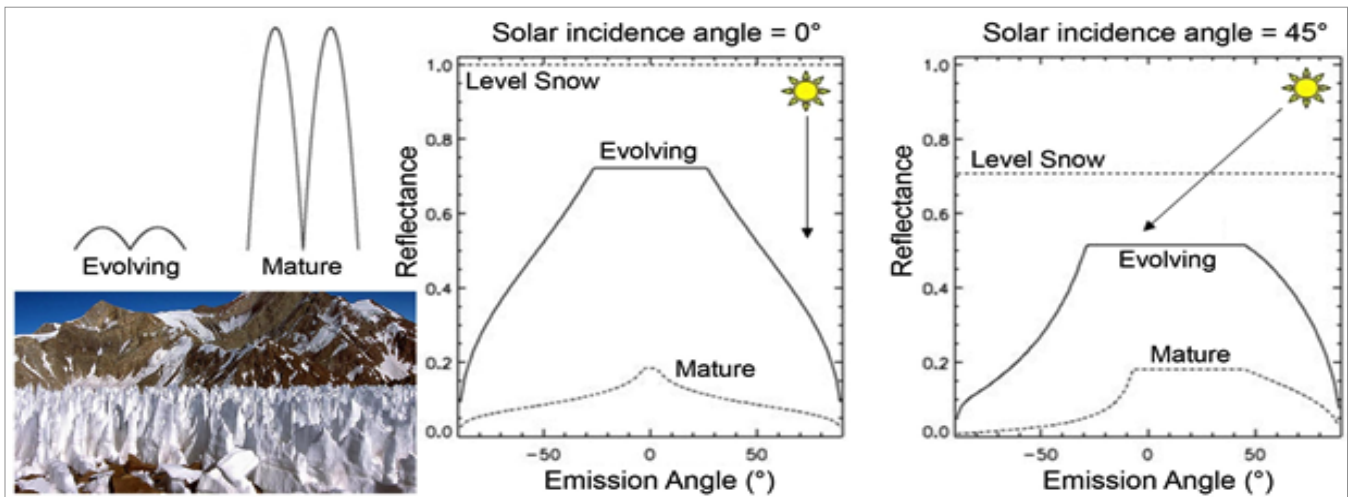

Figure 3. Evolving and mature ice pinnacle (penitentes) surfaces for solar incidence angles of 0° (left plot) and 45° (right plot) to illustrate extracting surface roughness from MUIR data. The height to width ratio is 0.5 and 5 for the evolving and mature models. The solid line is the reflectance that would be measured for the evolving model and the dash-dot line is the reflectance for the mature model. The dotted line shows a level snow or flat Lambertian surface.
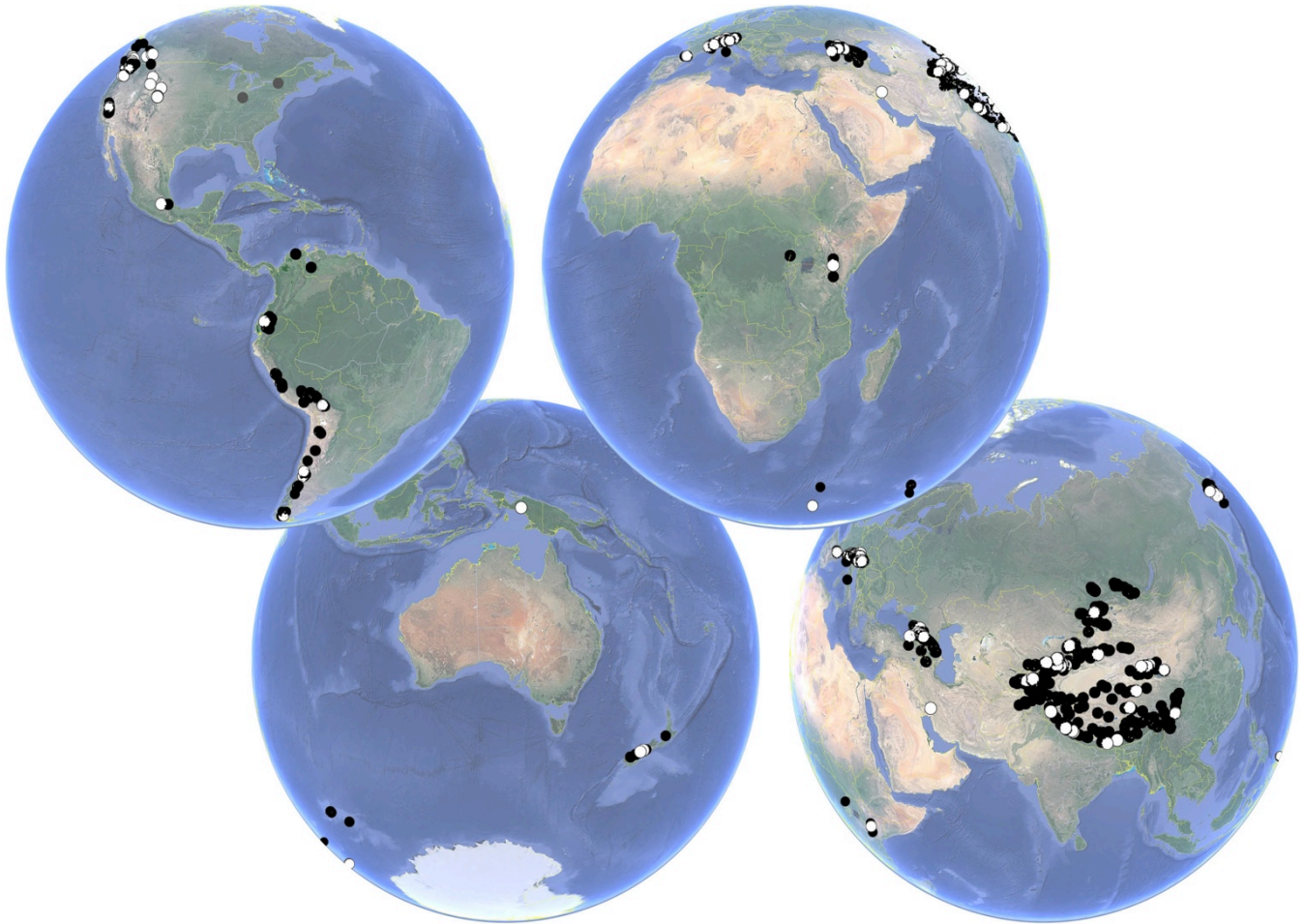
Figure 4. Geographically distributed representative target set for all regions with glaciers within latitude ±56° (black dots). 153 glaciers in that band have had mass balance estimates determined historically (white dots).

pinnacles, ponded water, wet ice, flat, and rough surfaces recognizable and quantifiable.

Staring at a target for up to a few minutes during a pass also makes it possible to observe rapid events in progress by capturing changes during a single pass. Areas prone to calving or avalanching could be targeted, increasing the probability of being observed as they occur. For example, iceberg drift could be tracked during a single pass. Icebergs sense different water depths depending on their size, so tracking a group of icebergs can provide information about stratification of currents, which are largely unmonitored despite their widely recognized influence on submarine ice loss and stability of tidewater glaciers.

Including a filter-wheel in front of a staring imager FPA enables high SNR spectral measurements without the typical compromise of spatial resolution. The color bands on push-broom sensors are very under-sampled, typically 3-4x coarser than their panchromatic band, to equalize the integration time. Even when a filter is in place, staring imagers will collect images at the full resolution of the optical system.

Moreover, tracking features over time enables characterization of changing and evolving ice surfaces that vary on diurnal to annual time scales. Staring imaging has

the capability to measure this variability and change on scales of minutes, months, and years. The goal of any staring measurements would be to have a repeat interval sufficient to capture short-term processes and a total mission duration long enough to capture longer term trends.

The ISS is a potential platform to host a staring instrument. We present here a point design for MUIR showing that it is feasible to mount a staring instrument on the ISS and recover sub-meter surface structure and albedo to an accuracy of 1%. The non-sun-synchronous orbit of the ISS meets the requirement for variable illumination of targets for different passes. The ISS is well suited for studying tropical and temperate glaciers between ±56° latitude. About 500 glaciers could be observed monthly and over 700 glaciers could be observed quarterly (Figure 4).

Staring-Mode Image Data Processing

Multiple image acquisitions during an overpass and pointing knowledge of each acquisition support advanced image processing methods that further augment the research capabilities of a staring imager. Digital photogrammetry and computer vision techniques, such as image super-resolution and structure-from-motion can be applied to create a three-dimensional model of the data for each color band [11, 12].

Table 1. Science traceability matrix. Studying response of mountain glaciers drives the need for a staring imager.

		Science Measurement Requirements		Instrument Requirements		Projected Performance 25 cm aperture on JEM-EF	Mission Requirements (Top Level)
Science Goals	**Science Objectives**	**Physical Parameters** spatial and temporal	**Observables**				
Determine the relative contributions of global and environmental change to the response of mountain glaciers	Determine glacier surface structure and variability	Glacier surface structure and changes	Raw imagery	Targets	≥350 quarterly	727 quarterly	Mountain glaciers
				Ground Sample Distance (GSD)	≤1 m/pixel nadir ground scale	0.8 m/pixel nadir ground scale	Geolocated context imagery
							3 year mission
				Spatial resolution	1 m	1.15 m diffraction/jitter limited	Staring capability
				Field of view	≥2x2 km at nadir	2.9 x 2.7 km at nadir	Multiple images per pass
			Correlated changes	Group motion of features	0.3 m/pair		≥4 collects/target/year
				Views per pass	40	40–380	Reconfigureable targeting
			Surface topography	Vertical elevation resolution	≤1 m (post-processed)	0.8 m (post-processed/pixel)	Tie points in image
				Field of regard	50° radius cone around nadir	60° along/ 50° cross track at nadir	Range of viewing angles
				Pointing	At nadir	At nadir	Non-sun synchronous orbit
				control knowledge accuracy jitter	150 m 200 m 250 m 50 cm	97 m 113 m 213 m 35 cm	Variable illumination
			Directional surface reflectance	Views per pass	≥10 each color	10-95 each color	
	Determine energy balance at the glacier surface	Glacier surface characteristics and changes		Reflectance (scene average)	SNR ≥100	SNR 100–170	
				Accuracy	2%	1%	Monochromatic imagery
				Multispectral	B, G, R, NIR	487, 562, 660, 835 nm	Four filters

This 3-D model is more complete than traditional stereo imaging because fewer areas are obstructed.

Generally, the improvement in spatial resolution under ideal conditions is approximately twice that of the individual data takes – for example, with 1-meter resolution, 0.5 meter resolved 3D models may be achieved. Radiometric resolution is also improved by merging multiple scenes. In a single-perspective image series (e.g. a series of nadir-viewing satellite images) the radiometry of an unchanging surface is improved by square root of the number of images used. This improvement is reduced somewhat by extracting higher spatial resolution and improved 3D rendering [13].

3. REQUIREMENTS AND ERROR BUDGETS

Volume changes and surface characteristics are needed to determine the relative contributions of global and environmental changes to the response of mountain glaciers (Table 1). By simultaneously measuring changes in glacier thickness and extent to infer mass balance and surface reflectance to infer glacier surface energy balance staring
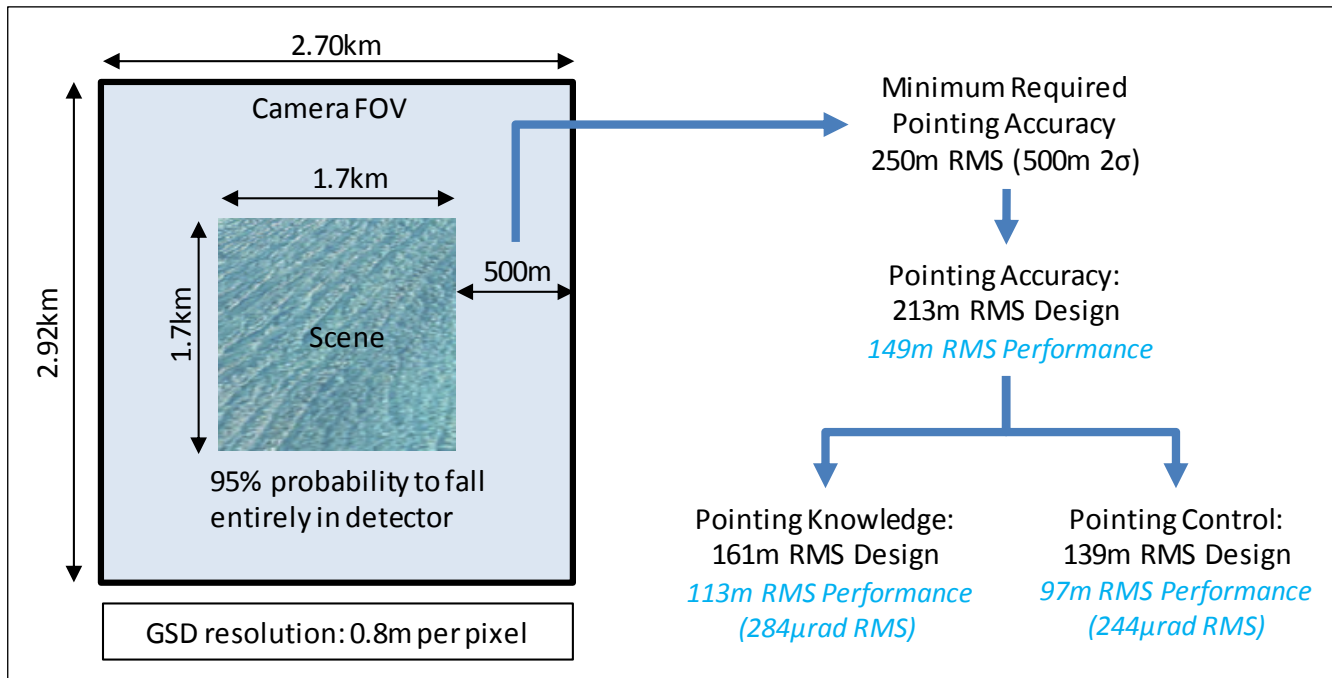

Figure 5. Pointing accuracy and field of view error budgets.

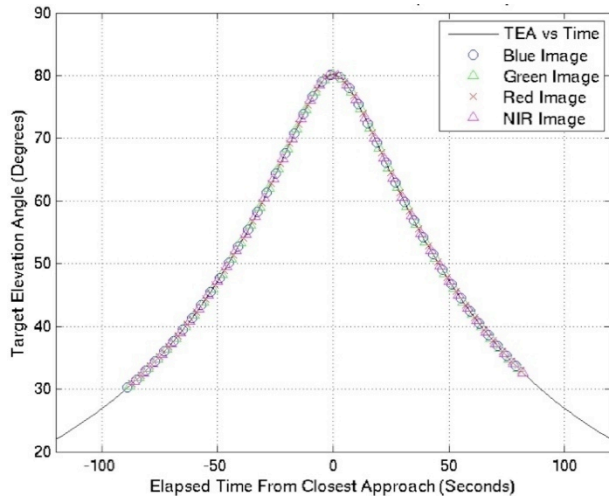imaging can be applied to determine the contribution of

Figure 6. MUIR observing profile showing time versus elevation angle. Image frame by filter is shown.

surface contamination to mountain glacier retreat. The key parameters required to meet these objectives are glacier volumes and surface characteristics and their variability in space and time. These parameters allow for the determination of changes in glacier volume and albedo. Spatially diverse measurements from variable illumination angles allow for much more complete 3D reconstruction and a truer measurement of reflectance and surface topology than standard imagery. Multispectral measurements improve the determination of surface material characteristics.

MUIR will characterize the 3D geometry of, and surface processes active on, mountain glaciers and correlate these processes to seasonal, environmental, and topographical variables. The instrument is designed to meet the resolution and rate requirements, and to acquire enough images through an acceptable range of angles to achieve required resolution for 3D recovery and BRDF determination. The imager Ground Sampling Distance (GSD) of 0.8 meter per pixel would result in a 2.9×2.7 km field-of-view. The pointing stability requirement of 0.5 meter Root Mean Square (RMS) and the pointing accuracy requirement of 250 meters RMS, both at nadir, would provide ≤ 1 m spatial resolution and guarantee $\geq 1.7 \times 1.7$ km fields of view for all the targets (Figure 5). Recovering 3D structure at 1 m resolution in all dimensions and surface reflectance to 1% requires 30 observations per channel equally distributed within a 50° cone around nadir, for a total of 100° and a ≥ 100 SNR.

Table 2. MUIR integration times for snow

Filter	Integration time for different solar zenith angles (in milliseconds)			
	0°	30°	45°	60°
Blue	7.9	9.8	12.1	18.9
Green	4.4	5.2	6.6	10.1
Red	6.1	7.1	8.9	13.1
NIR	9.7	11.3	13.9	20.2

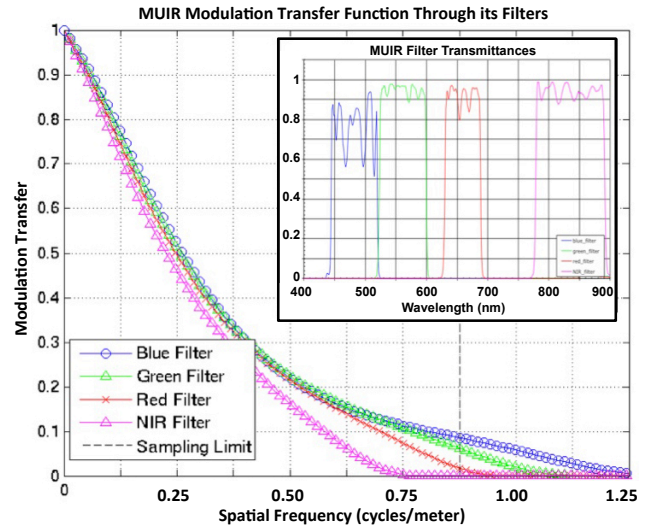Broad area mapping imagery collected from other sources

Figure 7. MUIR Modulation Transfer Function.

would provide context for MUIR's high fidelity 2.9×2.7 km field-of-view. An ideal feature of the ISS orbit is that it provides a non-sun-synchronous orbit, which is required to vary solar phase angles and illuminations for better recovery of surface characteristics.

Pointing and Geolocation
The MUIR gimbal system smoothly points the telescope at targets during passes. With its ±50° range of access it can provide up to 3 minutes of line-of-sight viewing to a point of interest and is able to hop between adjacent glacier scenes. The target elevation angle changes as a function of time (Figure 6). The instrument would rotate through its filter wheel, providing dozens of multispectral images from a large variety of perspectives. The gimbal encoder, combined with the on-board GPS and star tracker, would provide ~210 m absolute pointing capability, with ~160 m knowledge. This is sufficient for the science data system to co-register imagery of targets as big as 1.7 x 1.7 km with high probability of 95% (Figure 5).

System Throughput and Integration Time
Net filter throughput was analyzed using Modulation Transfer Functions (MTFs). Achieving SNR of 170 on snow as a function of solar zenith angle requires varying integration times (*Table 2*). Freedom to optimize the integration time for each band independently maximizes *SNR*.

Multispectral Image Quality
The spatial resolution of 1.14m is limited by diffraction and pointing disturbances as shown in Figure 9. The residual pointing jitter combined with the diffraction-limited performance of the optical system, would result in excellent image quality in all bands. MUIR imaging maximizes the resolution of the system with a Q > 1 based on the MTF (shown in Figure 7) which also minimizes the impact of

6

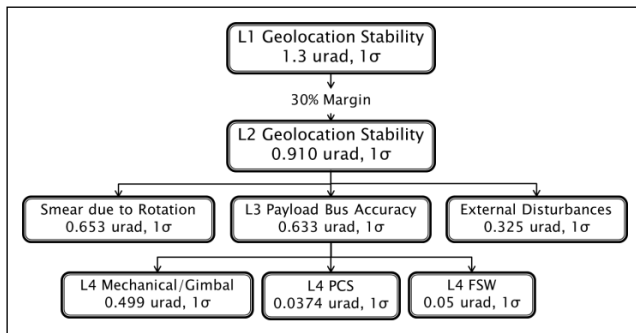aliasing in the imagery while maximizing the potential for information extraction.

Figure 8. Pointing stability error flow-down. The top-level allocation of 1.3µrad corresponds to the 0.5 meter projected on the ground at nadir.

The pointing stability requirement is driven by the need to limit image motion to less than 0.5 m RMS over the exposure time (up to 20 milliseconds). The pointing stability error budget (Figure 8) is calculated from three major sources: smear due to orbital rotation, jitter from rotation of the gimbal, and external disturbance. Jitter from rotation of the gimbal is the max angle swept during the image exposure time at the edge of the field of view. The external disturbance is calculated from integrating the ISS JEM-EF jitter power spectrum, developed by the OCO-3 project, over the exposure time. The mechanical jitter is calculated from measured open loop disturbance data of the JSC Robonaut dual stage-harmonic joint with 160-gear reduction, which is representative of the MUIR gimbal motor.

Multi-Angle Image Registration and 3D Recovery

Measurement of flow and volumetric changes requires resolving and tracking 3D glacier features over time. Detail in MUIR imagery allows co-registration of the images and recovery of features even for oblique images, which is fundamental to the 3D recovery process. These techniques have been successfully demonstrated through JPL's participation in the AFRL's Angel Fire aerial surveillance program. Reconstructed heights of buildings at Wright-Patterson Air Force Base have been verified where building volumes were correctly estimated to within 1%. MUIR multi-angle multi-frame collections result in finer estimates of the 3D structure while simultaneously solving for errors in the spacecraft ephemeris. Initial 3D structure is extrapolated using the known camera position and pose to triangulate the 3D facet and achieve sub-meter accuracy. Subsequent bundle adjustment computations refine the solution thereby reducing error in both the triangulated facets and spacecraft ephemeris. Vertical height resolution improves as the number of MUIR images increases (Figure 9), but more images increases computational needs. On a per-pixel basis, the system can achieve an optimal vertical height resolution of 0.7 meter with 30 images acquired from a 50° cone angle stemming from the target. Furthermore, the spatial diversity of the 30-image data set will improve reconstruction accuracy by increasing the likelihood of reconstructing facets occluded by surface features in some image segments. The precision of these estimates will improve linearly with the surface area for larger scale volumetric changes.

Surface Reflectance

Three tools for distinguishing snow, young ice, and mature ice are the brightness, color, and directionality of reflected
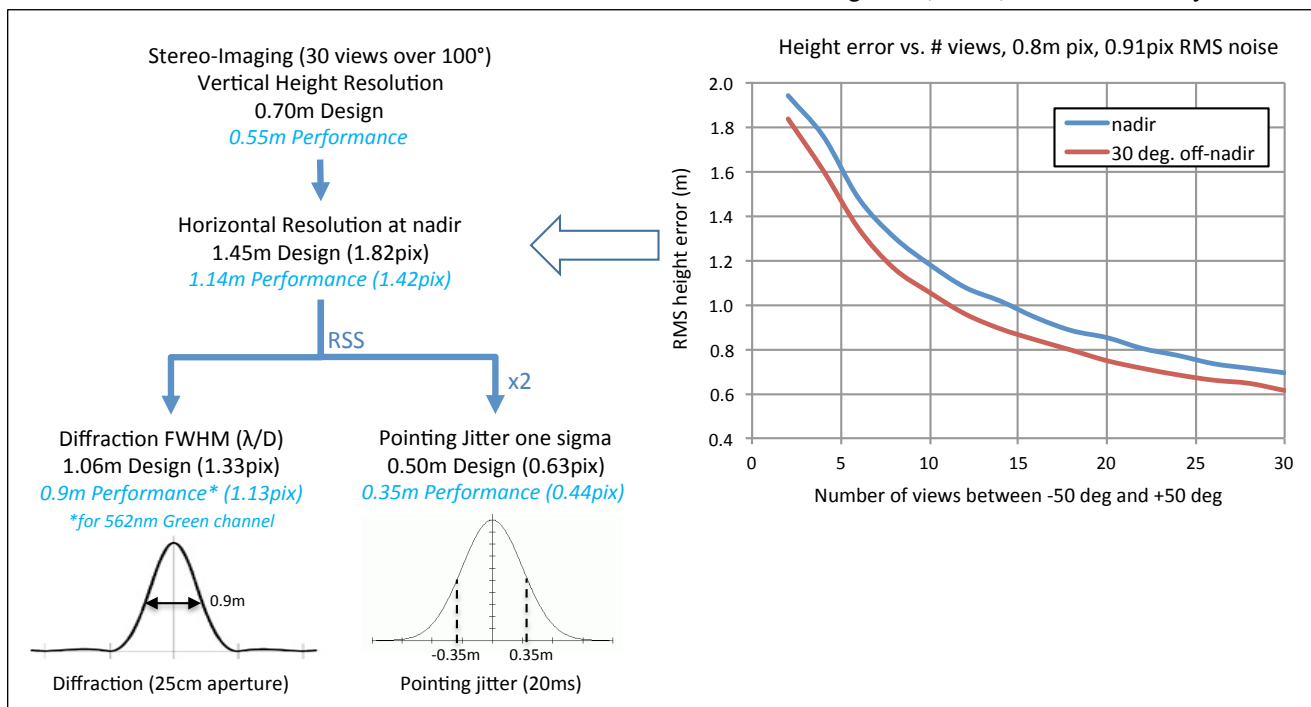

Figure 9. Imaging resolution error budget. Right Figure: height error versus number of views with 0.9 pixel RMS gaussian noise. Blue line is for nadir pointing and red line is for 30° off-nadir pointing.
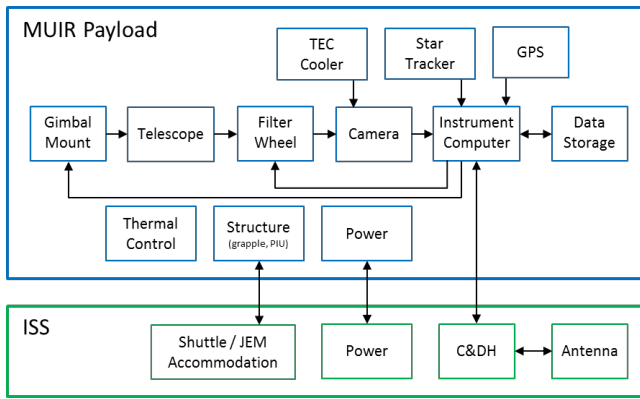
Figure 10. Payload block diagram accommodated on the ISS host platform.

light. Fresh snow is bright, white, and diffuse. Mature ice is darker, bluer, and more anisotropic. BRDF resolution is a few times the DEM resolution; the BRDF requires a local slope vector determined from at least three DEM points defining a facet. Four points in the DEM grid that define two triangular facets produce a BRDF resolution twice the resolution of the DEM. 0.8m DEM points result in 1.6 m BRDF resolution. Photometric accuracy of the BRDF is the Root of Sum of Squares (RSS) of the SNR for a single image divided by the square root of the number of images per pass. For 10 images per pass per filter, with SNR of 100 in each filter, the BRDF accuracy is 0.3%, which exceeds the requirement of 2%. Accurate determination of the local surface normal requires more than this minimum number of DEM points trading photometric accuracy for BRDF spatial resolution.

4. IMAGER DESIGN

The MUIR staring imager draws on the heritage of the AFRL Angel Fire platform that has been successfully used to extract structure from motion from airborne imagery. The instrument and its components would acquire many high-resolution images of a target from many vantage points during an orbit pass in order to adequately resolve surface characteristics and structure. The key components of the instrument are the telescope, detector, filter wheel, star tracker, and gimbal that make up a single, stable, imaging instrument that will provide near diffraction limited images of ground targets collected from a range of angles (Figure 10).

Telescope

The telescope for this point design is a 25cm aperture un-obscured Three-Mirror Anastigmat (TMA; Figure 11). The TMA is diffraction limited, with a Strehl ratio of 0.94 or greater across the required field of view and wavelength range. The athermal, all-aluminum, telescope implementation is based on previous flight designs using L3-Tinsley's mirror manufacturing process. It would be aligned and operated near room temperature and would be further athermalized by the all-aluminum construction. A telescope baffle would provide thermal shielding, reduce

stray light, and increase viewing angles relative to the sun. The telescope is a passive design with no fine steering mirror or focusing mechanism. The active thermal control system would mitigate thermal gradients across the telescope. Multispectral imaging would be accomplished with a geared stepper motor filter wheel that adopts the MER PanCAM design. Four color filters would be centered
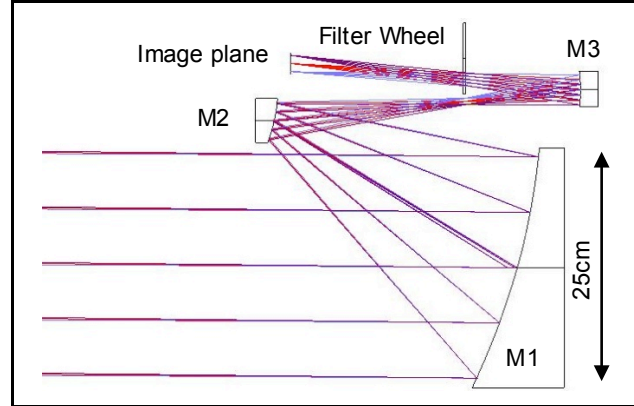

Figure 11. Instrument ray trace.

at 487, 562, 660 and 835nm and located at the intermediate pupil (Figure 2).

Focal Plane Array

The selected Focal Plane Array (FPA) would be a BTBV12M CMOS detector, manufactured by Teledyne and packaged by JPL (Figure 12). The BTBV12M is a high performance low cost 3375×3648 pixels front-illuminated monolithic imager with an all-digital interface that is significantly faster than analog output imagers such as CCDs. MUIR would operate the detector at two full frames per second, achieving the required coverage and minimizing read noise. The FPAs should be subjected to rigorous flight qualification testing, and also provide calibration data for post-processing.

Mechanical

The MUIR payload could be installed on the Japanese Experiment "Kibo" Exposed Facility (JEM-EF), at any of the EF Standard Experimental Payload sites, 1, 3, 4, 5, 6, or 8. The payload can be installed on either the Ram or Wake side of the JEM-EF. The field of view (FOV) of the telescope is currently symmetric in the Nadir direction but the star tracker is not due to field of view constraints. The mounting bracket would need to be tailored pending installation location. The payload is designed to the standard electrical interface of the JEM-EF 120V lines for both operational and heater power. The payload could interface

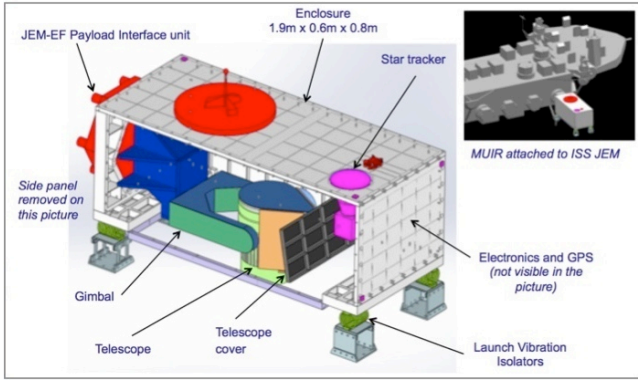**Figure 12. Packaged BTBV12M detector from Teledyne.**

8

Figure 13. Configuration drawing showing internal parts and instrument attached to the ISS JEM

with the standard 1553 and Ethernet. The payload does not require the available cooling loop as it has its own independent thermal management system.

The JEM-EF sites provide the best options for the telescope FOV facing nadir and the star-tracker FOV facing Zenith. The payload could be accommodated on the nadir facing ELC FRAM sites however with degraded performance due to the obstructed view of the star tracker in the zenith direction. A second star tracker could be added at additional cost to accommodate the ELC FRAM locations. The total CBE mass is 312kg; only 60kg is actual instrument mass and the other 252kg mass is used to maintain the established interfaces for the JEM-EF, robotic arms, and launch vehicles. The CBE mass of 312kg is well within the 500kg allocation of the JEM-EF standard payloads, but the 60kg instrument mass would be capable of being accommodated on the ELC sites 1 and 4 with a much smaller interface structure since the FRAM provides all of the structural rigidity and attachment points for the ISS interfaces.

The instrument for this point design is housed in an aluminum box that provides a thermal and mechanical barrier from outside disturbances. This structure is the main load path between the two robotic grapple fixtures, JEM-EF Payload Interface unit (PIU), launch vehicle adaptors and other payload subsystems, including gimbal, star tracker, GPS and avionics box. The design (Figure 13) draws heritage from the OCO-3 mechanical design. The nadir panel of the main structure remains open to allow an un-obstructed view of the Earth. The size and mass of the structure is driven by JEM-EF payload related requirements for the ISS. Much of this structural mass would be eliminated in a free-flyer implementation.

Within the main structure, the mechanical subsystem is a two-axis direct-drive gimbal that provides ±60° along track along the ISS velocity vector and ±50° in the cross track direction (Figure 14). During an ISS overpass, the gimbal rotates the telescope to track and stare at a ground target. The gimbal electronics receives a command profile from the pointing and control system and regulates the power to the motors by closing the loop around high-resolution encoders to maintain the appropriate accuracy. The gimbal design
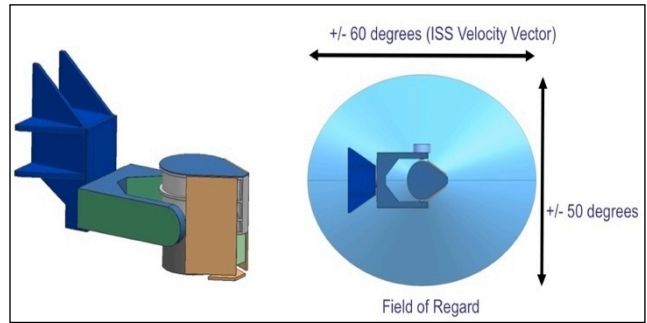

Figure 14. MUIR two-axis gimbal with telescope (left) and the gimbal field of regard (right).

incorporates zero-cogging brushless DC motors with a large gear reduction to keep the pointing disturbances low and meet stability requirements.

Thermal

The thermal control of the MUIR instrument is divided into four main zones: the optical barrel, the gimbal, the electronics, and the focal plane. The thermal design is biased toward the cold range of allowable flight temperatures (AFT) using a large radiator for the electronics and tailored surface coatings with white Beta cloth multi-layer blankets for the other zones. Heaters are used to maintain control at the lower AFTs.

The thermal design was developed within the JSC Thermal Desktop model of the completed ISS with the instrument installed in the JEM-EF. Instrument performance was studied for the full range of beta angles and hot/cold thermal environments. The variable heat-load and camera articulation were included in the model. The all-aluminum telescope design meets the requirement of 1°C temperature stability and gradient (Figure 15). Four heater zones are utilized on the optical barrel in order to reduce the temperature gradient. During operation, instrument temperature is stabilized with sixteen proportional-integral-derivative controlled heater zones using a maximum of 230W of total power. The star tracker temperature set point
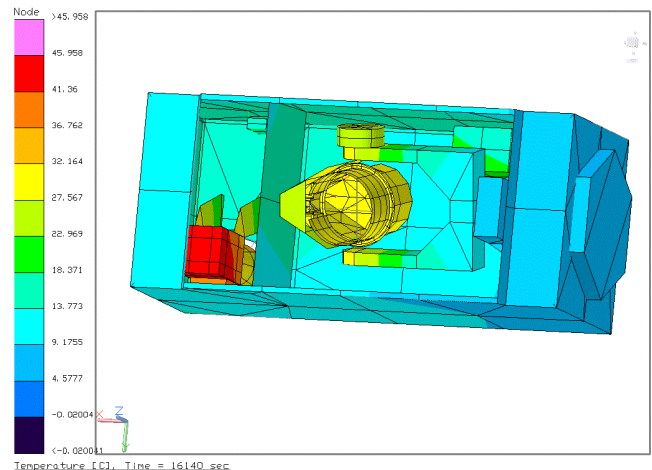

Figure 15. Predicted temperature from the instrument thermal model for a typical hot case.
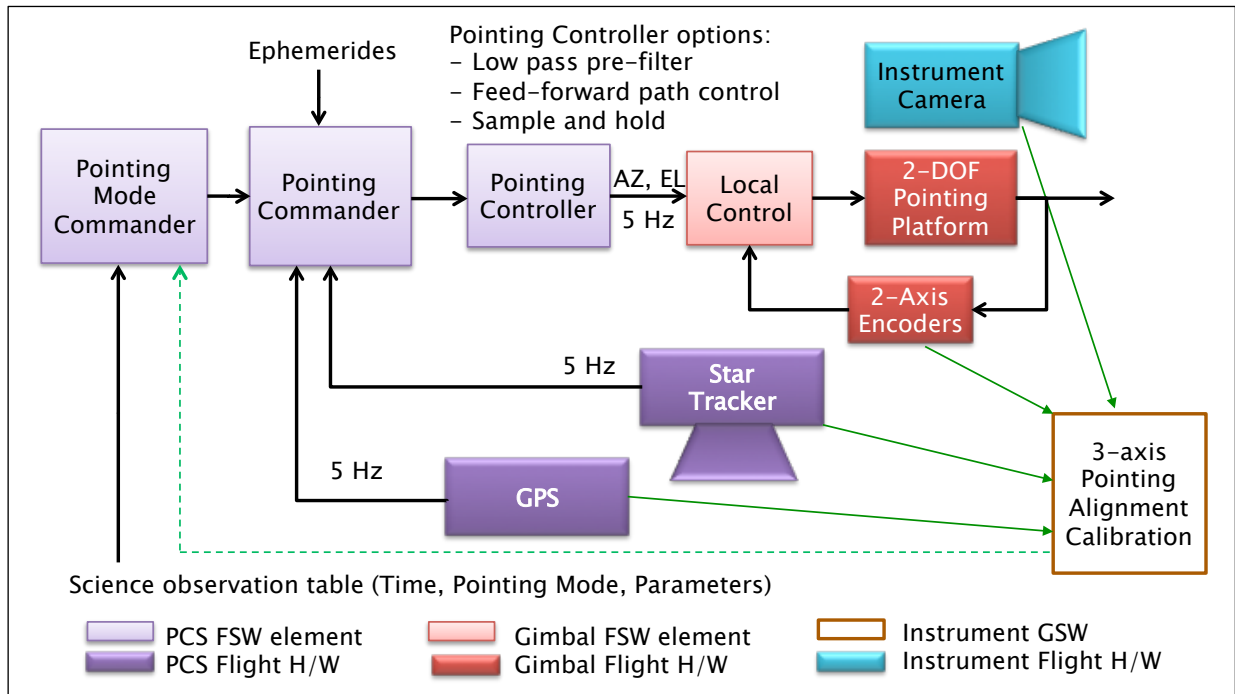
Figure 16. Pointing control system block diagram.

is 40°C to speed recovery from sun exposure during orbits with low beta angles.

Selective use of phase-change heat sinks maintains the temperature of more sensitive components like the star tracker. An off-the-shelf thermoelectric cooler would provide 6 W of cooling to maintain the detector temperature at $0 \pm 1°C$ throughout the variable thermal environment. Radiators would be mounted on the side of the telescope.

Pointing & Control System

The Pointing and Control System (PCS) architecture is composed of one star tracker and one GPS unit, which are used to provide the inertial attitude and position estimate of the payload (Figure 16). The star tracker is the Sodern SED26 commercial unit and the GPS is the Surrey SGR-20 commercial unit. Changes to the attitude are implemented through the gimbal system. Periodic calibrations to the instrument will be performed to remove bias and misalignments between the sensors and the gimbal. The PCS provides a target path to the gimbal system based on the attitude estimate from the star tracker. The system is robust to GPS outages of up to a couple of minutes by using the ISS orbit ephemerides to propagate the state. This architecture is identical to the Orbiting Carbon Observatory 3 (OCO-3) PCS, which provides both technical feasibility and heritage.

Electronics and Software

The electronics chassis contains a power conversion board, an analog power supply, a RAD750 processor board, a mechanism control board for the filter wheel, gimbal, thermo-electric cooler (TEC), and heaters control, a digital interface board for the focal plane, star tracker, and GPS

I/O, 128GB of flash memory for data storage, and an Ethernet interface to the ISS for command, telemetry, and science data (Figure 17). All circuit designs have been flown before resulting in high Technology Readiness Level (TRL).

The field programmable gate array (FPGA)/flight software (FSW) functions control the filter wheel mechanism, set up the heaters and the FPA cooler, monitor the health and safety of the instrument, and accept commands from the ISS that require changes of the operating conditions. Housekeeping data should be provided periodically. The focal plane data, collected and stored in the instrument flash memory, would be transmitted with the negotiated rate by handshaking, which is managed by the FPGA/FSW using a table driven operation. FSW should be built and tested iteratively, implementing highest-risk algorithms first, followed by added functionality with successive builds.

5. CONCEPT OF OPERATIONS

The mission operations system (MOS)/ground data system (GDS) architecture includes the personnel and software interfaces with the HOSC POIC, payload monitor and control integrated into automated planning and execution, and ground data management, including science data processing (Figure 18). After an initial checkout period, MUIR would make continual observations of glacier targets. The priority of a target should be determined to maintain the required image cadence, likelihood of cloud cover/ occlusion, and availability of targets of interest. Data downlink would occur asynchronously, usually during the dark portion of the orbit. Stowed-calibration events also occur during the dark portion of the orbit to avoid conflicts with science observations.
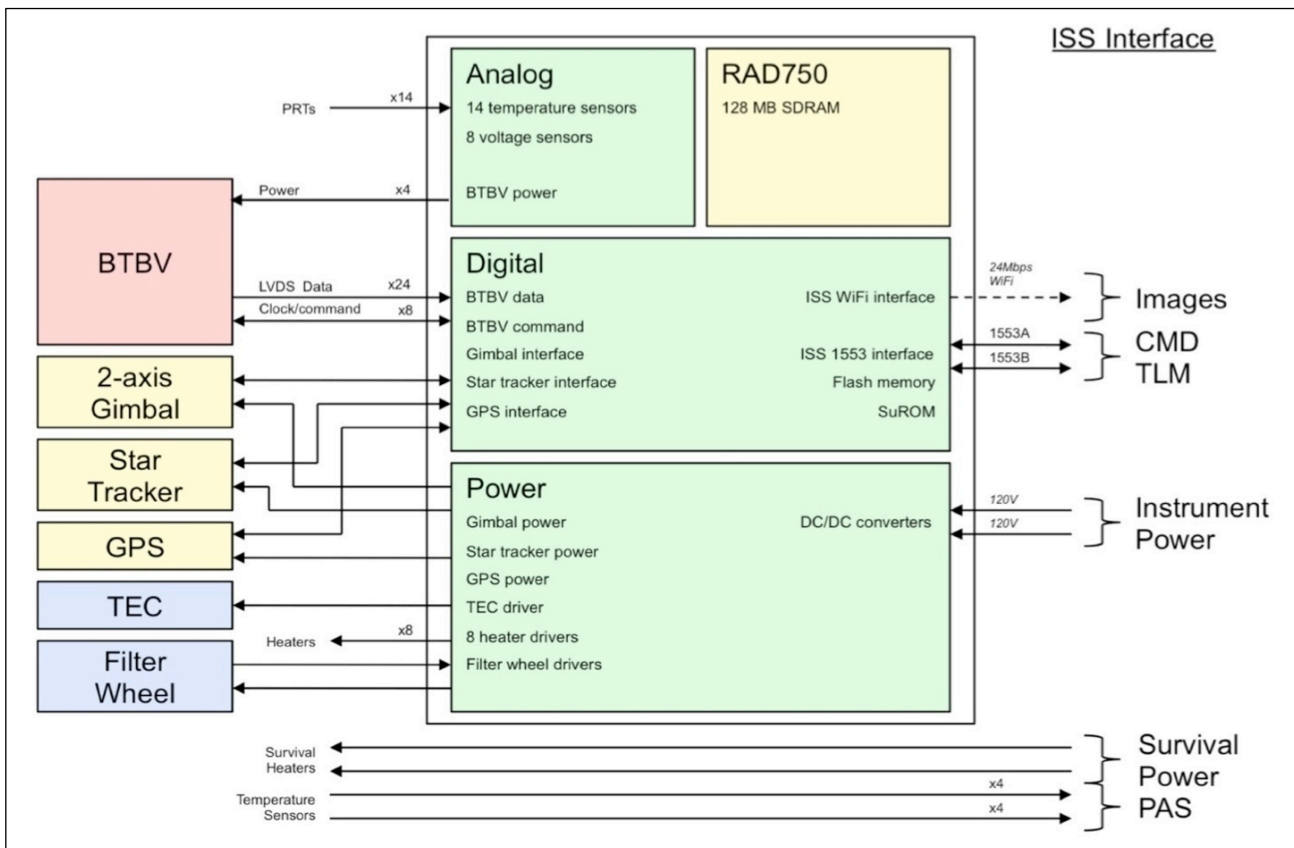
Figure 17. Electronics block diagram.

Science Operations

Operational modes consist of single target imaging, pair target imaging, idle, and stowed (Figure 19). During a pass MUIR will take a series of images of a target while cycling through the four filters. Single target mode maximizes the number of images for that target during a pass; a target is acquired and tracked for a maximum of 120°. Two targets per orbit is typical. Pair target mode maximizes the number of targets allowing alternating imaging of a second target within 20km of the first. Idle mode occurs when the instrument is not imaging but not stowed. Non-uniform glacier distribution over the globe results in significant idle time of about 60% of the day time of the instrument, which could be used for other investigations. In stowed mode, the instrument points to a calibration target inside the enclosure.

Operations are responsive to unforeseen or unpredictable events that demand response as soon as possible. Image targets can be integrated with the onboard plan as soon as possible. The scheduling is performed automatically on the ground with inputs that include current expected cloud cover and spacecraft ephemerides. While MUIR would always fly a full day's worth of observations, the plan could be updated on every orbit. The system automatically re-plans around any perturbation of the schedule and operations staff can insert new goals into the system. This ability to replan with short deadlines is already part of the concept of operations for missions such as RapidScat. By 2017 the ISS will likely have a Ku-forward capability that provides a standard for closed loop commanding.
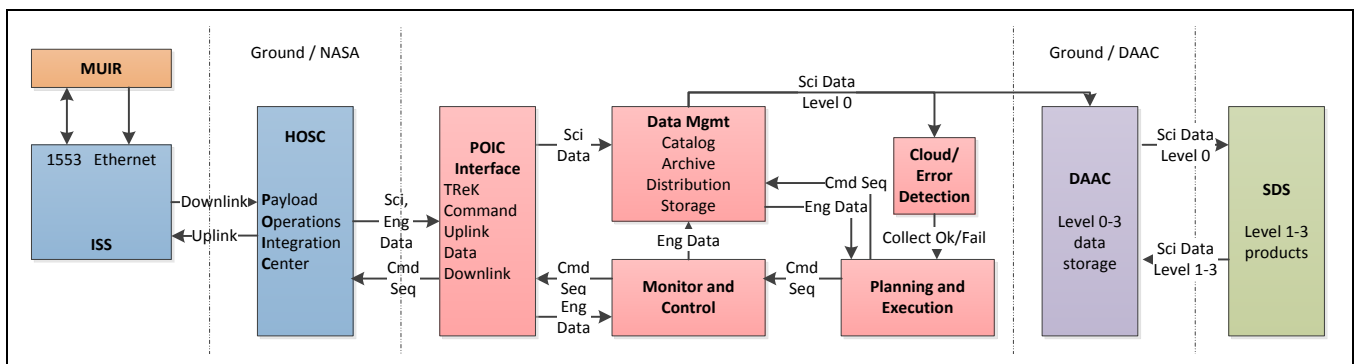
Data would be written to onboard storage and downlinked

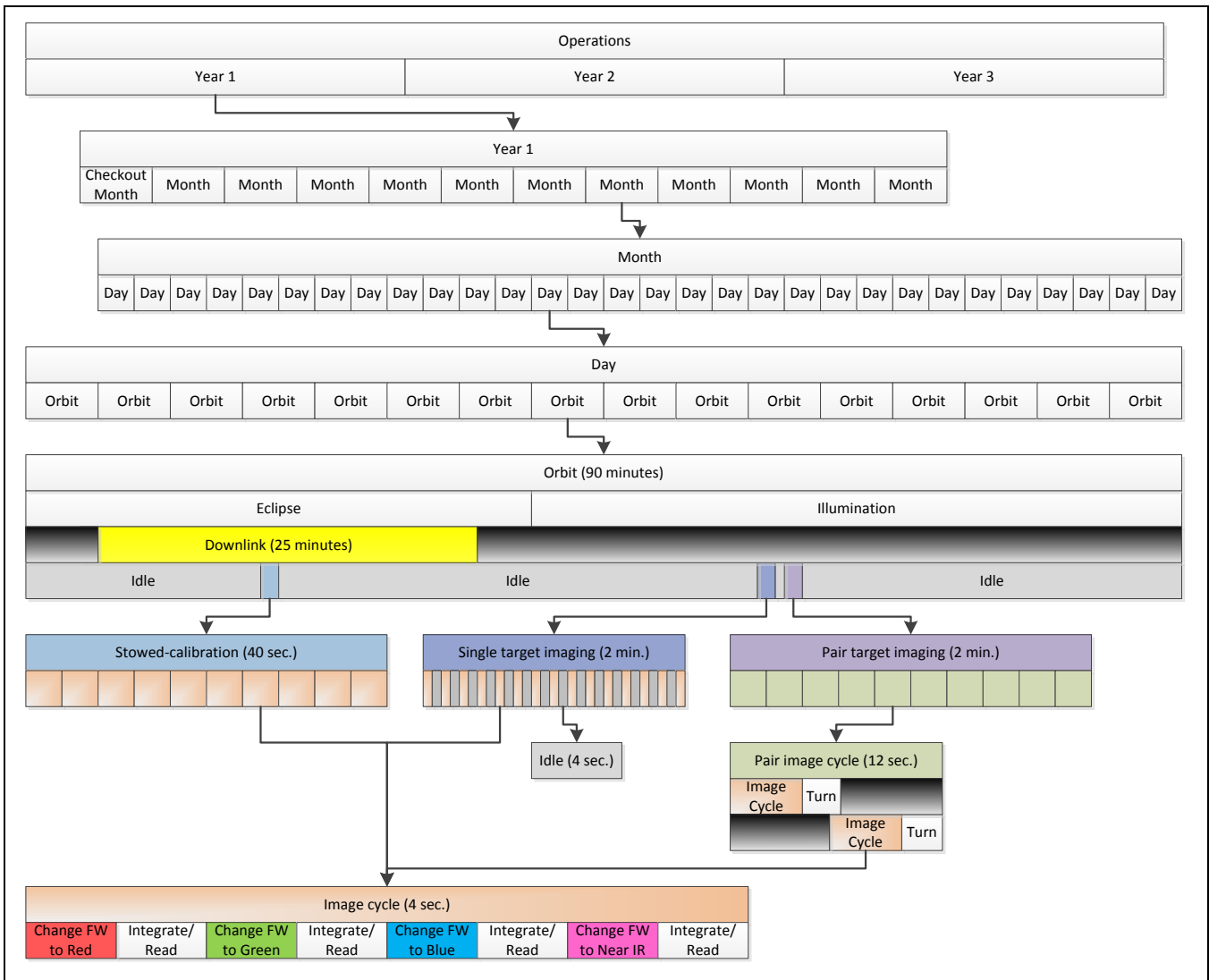

Figure 18. MOS/GDS Architecture

Figure 19. MUIR Operational Mode Schedule

during dark side passes. Average downlink accommodation is 3Mb/s and downlinks are typically of 25-minute durations at 10Mb/s. Daily data production, after compression, is 9.8GB, assuming a 3:1 compression ratio similar to what is routinely achieved for EO-1. On-board storage is sized at 128GB, providing for 13 days of on-board data buffering. Data products would be validated on the ground and station operations can impose blackouts.

Calibration/Validation Approach

Calibration and validation are required for the components, instrument, measurements, and algorithms to ensure the accuracy and precision needed to deliver data products at the required performance. Calibration and validation will occur during I&T and on-orbit check-out, but will also be conducted periodically to maintain product performance and optimize operations.

On orbit, the single defined calibration mode is Stowed-Calibration. The telescope points to its cover when stowed. By illuminating and imaging the cover using different integration times, the system flat-field gain, offset and dark maps are derived and updated.

Instrument level calibration will be verified by imaging dry lakebeds and salt flats that have been ground truthed. Observations of established and well-characterized ground targets are planned for the geolocation, resolution, 3-D reconstruction, and radiometric calibrations as well as DEM retrieval verification. Imaging known targets would enable an assessment of the MUIR MTF and provides stable fiducials for geolocation and volumetric reconstruction verification. Acquiring images of smooth, bright targets concurrent with ground-based radiometric measurements is another on-orbit radiometric calibration activity.

Science Products

The ground data system is designed to automatically apply a series of calibrations and processing to the raw instrument data and metadata (Figure 20) and would produce the following products:
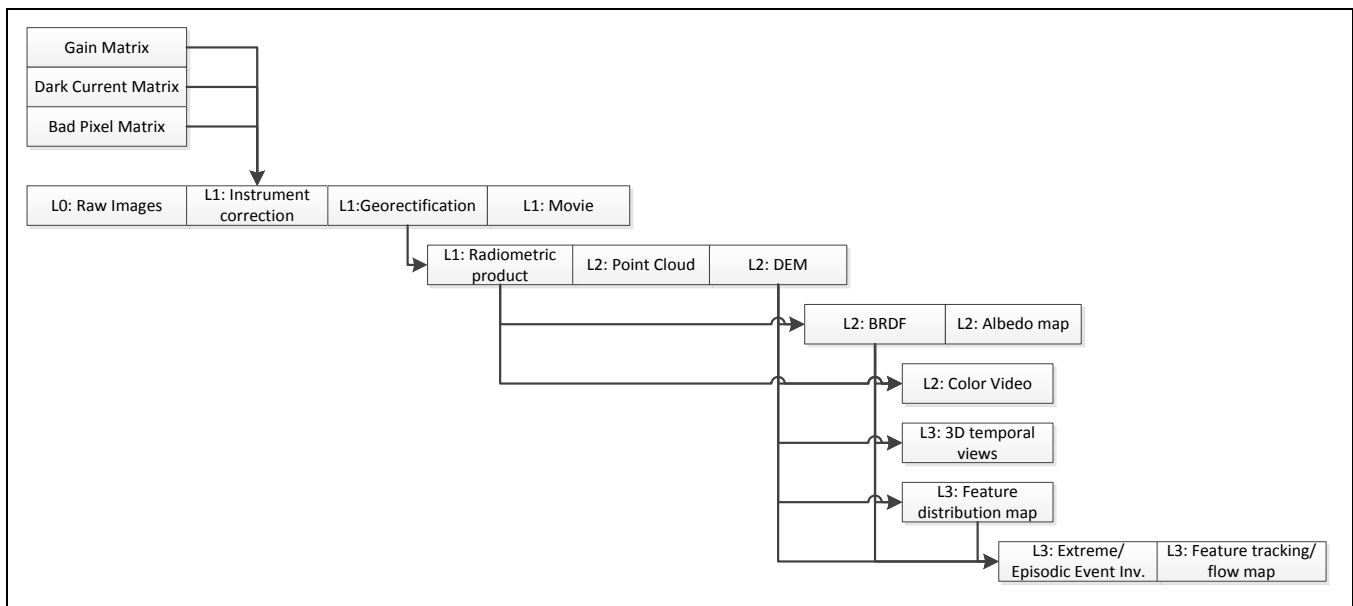
Figure 20. Processing flow of the product generated in the MUIR ground data system.

Level 0 – Raw images and metadata: Image metadata includes time, target, pass identification, filter, detector temperature, ephemerides, pointing, camera orientation, star tracker information, sun elevation and azimuth.

Level 1 – Optically, geometrically, radiometrically corrected images and movies: processing includes instrument corrections, which are dark current subtraction, flat-fielding, bad pixel removal, and camera field distortion correction. A radiometric correction converts the signal in each pixel to physical units of radiance. For Level 1 products each pixel is assigned geographic coordinates, photometric coordinates, and radiance. Images are co-registered and georectified using WorldView2 (and WorldView3) observations of targets collected 1–2 times per year. The images are combined into a movie for a quick-look summary of the pass over each glacier.

Level 2 – Multispectral (Color), DEM, BRDF, albedo retrieval products: processing combines images from 1 to 3 passes, each corresponding to a different solar incidence angle on different orbits to produce a DEM. 'Point clouds' are the dense set of derived 3D points (one per rectified pixel) tracked over a pass and in-between passes and is a precursor product to DEMs. The point cloud and DEM are archived to efficiently track long-term changes and surface displacements.. The derived DEM will determine the local normal vector to each triangular facet composed of three georectified positions in the scene. BRDF measurements for each facet are proportional to the radiance at each geometry and should be archived. Spectral albedo for each filter and incidence angle is the integral of the BRDF over all emission and azimuth angles. The albedo defining the total fraction of solar radiation reflected is the integral of the spectral albedo over wavelength weighted by the solar irradiance. Albedo and spectral albedo for each facet should be archived.

Level 3 – Multipass temporal products quantifying volumetric changes and systematic flow: products model the L2 products to map surface characteristics and combine results from many passes to focus on the temporal evolution of glaciers. From the spectral and angular variation of the BRDF, maps of surface types including ice, snow, albedo debris cover, unresolved roughness, and surface water would be generated. Color images and movies of each glacier would be created to help visualize the changes during the mission.

6. DISCUSSION

The International Space Station (ISS) provides a suitable host for an instrument to conduct staring observations of mountain glaciers. From the ISS it would be possible to observe hundreds of tropical and temperate glaciers in the ±56° latitude band. These glaciers are particularly sensitive to global and environmental change because they are near the melting point of ice and their surfaces can gather dust and soot causing increased melt and exacerbating glacier retreat. A limitation of the ISS as a host platform is that it is not possible to observe some of the many retreating mountain glaciers in Alaska, Arctic Canada, Iceland, and the Russian Arctic. However, systematic measurements probing surface characteristics and processes could be made for many glaciated regions that have thus far received little systematic attention.

The point design presented here has a gimbal that can accommodate motion and jitter of the ISS as the instrument stares at a target during a pass. A sampling strategy that increases the number of targets uses the gimbal to switch back and forth between glacier targets during a pass. A fast steering mirror in the telescope could enable more measurements of glaciers during each pass.

13

The field of view of the instrument is >2 x 2 km at nadir, caputring the width of most mountain glaciers; 92% of glaciers in ±56° latitude are <1 km wide and 59% are <1 km long. An additional 25% are <2 km long. The 25 cm aperture and ISS mounted payload result in 1.15 m diffraction and jitter limited resolution performance. 50 cm resolution would better resolve fine features such as boulders and crevasses. The Express Logistic Carrier (ELC) sites on the ISS could accommodate a larger telescope. Additional jitter mitigation would need to be implemented to benefit from the improved resolution. Accommodating the MUIR instrument on a free flyer would be another way to increase the aperture, thus improving resolution while keeping a sufficient field of view for characterizing the typical small footprint of mountain glaciers.

7. CONCLUSIONS

Staring imaging provides a means of measuring detailed surface structure and reflectance. For glaciers, staring imaging can be used to simultaneously infer mass and energy balance. Staring at a few multispectral bands can aid in inferring material properties of the surface. The ISS provides a suitable host platform for a staring instrument payload, which could be mounted on the JEM-EF facility. A staring instrument that provides measurements from multiple viewing and illumination angles enables simultaneous measurement of 3D surface structure, including texture, material characteristics, and albedo, making it possible to determine and understand rates and patterns of melt from absorbed solar energy. The non-sun-synchronous orbit of the ISS enables varying solar illumination angles, and a staring instrument mounted on the ISS would access all tropical and most temperate mountain glaciers.

REFERENCES

[1] Gardner, A.S., G. Moholdt, J. Graham Cogley, B. Wouters, A.A. Arendt, J. Wahr, E. Berthier, R. Hock, W. Tad Pfeffer, G. Kaser, S.R.M. Ligtenber, T. Bolch, M.J. Sharp, J. Ove Hagen, M. R. van den Broeke, F. Paul (2013), A reconciled estimate of glacier contributions to sea level rise: 2003 to 2009, Science, 340, 852–857, DOI: 10.1126/science.1234532.

[2] Meier, M.F. (1984), The contribution of small glaciers to sea level rise. Science, 226, 1418–1421.

[3] Barnett T.P., J.C. Adam, D.P. Lettenmaier (2005), Potential impacts of a warming climate on water availability in snow-dominated regions. Nature, 438, 303–309.

[4] Gardner, A., and M.J. Sharp (2010), A review of snow and ice albedo and the development of a new physically based broadband albedo parameterization, J. Geophys. Res., 115, DOI : 10.1029/2009JF001444.

[5] Bridges, N.T., P.E. Geissler, A.S., McEwen, B.J. Thomson, F.C. Chuang, K.E. Herkenhoff, L.P. Keszthelyi, and S. Martinez-Alonso (2007), Windy Mars: A dynamic planet as seen by the HiRISE camera, Geophys. Res. Lett., 34, DOI: 10.1029/2007GL031445.

[6] Bagnold, R.A. (1954), The Physics of Blown Sand and Desert Dunes, republished by Dover 2004, ISBN 13:978-D-486-43931-0, 266 pp.

[7] Koudelka, M. L., Magda, S., Belhumeur, P. N., & Kriegman, D. J. (2003, October). Acquisition, compression, and synthesis of bidirectional texture functions. In 3rd International Workshop on Texture Analysis and Synthesis (Texture 2003) (pp. 59-64).

[8] Dana, K.J., B. Van Ginneken, S.K. Nayar, J.J. Koenderink (1999), Reflectance and Texture of Real-World Surfaces, ACM Trans. on Graphics, 18, 1–34.

[9] Hall, D.K. and J. Martinec (1985), Remote sensing of ice and snow. Chapman and Hall, New York, 189 pp.

[10] Westoby, M.J., et al. (2012), "Structure-from-Motion" photogrammetry: A low-cost, effective tool for geoscience applications, Geomorphology, 179, 300–314.

[11] Ekholm, J. (2012), 3-D Scene Reconstruction from Aerial Imagery, Thesis, Air Force Institute of Technology, AFIT/APPLPHY/ENP/12-M03.

[12] Marques, M., & Costeira, J. (2008, January). Optimal shape from motion estimation with missing and degenerate data. In Motion and video Computing, 2008. WMVC 2008. IEEE Workshop on (pp. 1-6). IEEE.

[13] Scambos, T. A., Kvaran, G., & Fahnestock, M. A. (1999). Improving AVHRR resolution through data cumulation for mapping polar ice sheets. Remote sensing of environment, 69(1), 56-66.

BIOGRAPHIES

Andrea Donnellan *is a principal research scientist at NASA's Jet Propulsion Laboratory, and Adjunct Assistant Professor of Research of Earth Sciences at the University of Southern California. She is President-elect of AGU's Nonlinear Geophysics Focus Area and is Principal Investigator of NASA's QuakeSim project, which was co-winner of NASA's 2012 Software of the Year Award. Donnellan was Deputy Manager of the JPL's Science Division, Pre-Project Scientist of an L-band radar mission, and NASA's Applied Sciences Program Area Co-Lead for Natural Disasters. Donnellan received a B.S. in geology from the Ohio State University in 1986, a master's and Ph.D. in geophysics from Caltech in 1988 and 1991 respectively, and an M.S. in Computer Science from the University of Southern California in 2003.*

Bruce Bills *is a research scientist at the Jet Propulsion Laboratory. His research focus is geodynamics of solid planets, satellites, and asteroids. He received a B.S. in mathematics and physics from Brigham Young University in 1973, and Ph.D. in planetary science from Caltech in 1977.*

Joseph J. Green *is a senior optical engineer at NASA's Jet Propulsion Laboratory. For the past 13 years, he has advanced the state of the art in wavefront sensing and control, active optics, high-contrast imaging and image processing on many projects including JWST, TPF, SIM and Spitzer. In 2007 he was part of the JPL team that won the NASA Software of the Year Award for their MGS wavefront sensing software. In 2008, he received the JPL Explorer Award for excellence in his image processing work with a reimbursable customer. Dr. Green received his BS in electrical and computer engineering from the University of Michigan (Dearborn) in 1994 and his MS and PhD in electrical and computer engineering from the University of Arizona in 1997 and 2000 respectively.*

Renaud Goullioud *is a principal systems engineer at the Jet Propulsion Laboratory and has over 15 years of experience in systems engineering and management of complex optical instruments for astronomy and Earth science. He has an EE degree from the Institute of Chemistry and Physics of Lyon, France, and a Ph. D. in electronics from the National Institute of Applied Sciences of Lyon. He has worked on NASA's Space Interferometry Mission from 1997 to 2010 and has received the NASA Exceptional Technology*

Achievement Medal in 2006, for leadership of three of SIM's major technology testbeds, whose successful completion played a critical role in establishing technology readiness for the mission. Recently, he was the Project Systems Engineer for OpTIIX, a class D technology demonstration for a segmented mirror space telescope to be installed on the ISS.

Susan Jones *is a systems engineer in the Project Systems Engineering & Formulation section of the Jet Propulsion Laboratory. Susan has 30 years of experience at JPL including systems engineering and architecture development for collaborative engineering systems, pre-project information systems, and technology management systems. She has managed the operations of JPL's Team X Project Design Center and has provided Mission Planning and Mission Operations System (MOS) design for NASA projects such as Magellan, Topex/Poseidon and the Shuttle Imaging Radar/Synthetic Aperture Radar Project (SIRC/XSAR). She earned her B.S. in Aeronautics and Astronautics at the University of Illinois, Urbana-Champaign.*

Russell Knight *is a principal technologist at JPL and is the cognizant engineer for CASPER, an embedded real-time planner and scheduler, which is a component of ASE, the 2005 co-winner of the NASA Software of the year award, and flying on EO-1. He is the inventor of CLASP, an area-coverage planner. Knight has a B.S. in computer science from the University of Maryland and a M.S. and Ph.D. in computer science from the University of California, Los Angeles.*

Michael Underhill *is a Mechanical Engineer at the Jet Propulsion Laboratory. Over the past 6 years his work has focused on designing, building and implementing precision two-axis gimbals for space flight. He received his B.S. degree in Mechanical Engineering and Business and Economic Management at the California Institute of Technology in 2008.*

Jay Goguen *is a research scientist in the Asteroids, Comets & Satellites Group in the Science Division at JPL. He received a B.S. in Physics from the University of Massachusetts (Amherst) and graduated Magna Cum Laude in 1974. He received an M.S. and Ph.D. in Astronomy & Space Sciences from Cornell University in 1977 and 1981. He held a National Research Council Postdoctoral Fellowship at JPL from*

1986 to 1988 when he converted to a full-time employee of JPL. Jay's research interestes include physics and chemistry of ices and their relationship to remote sensing measurements, modeling radiative transfer in planetary surfaces, quantitative interpretation of photometry, polarimetry and spectroscopy of solar system objects, measurement and analysis of the thermal emission from Io's volcanos, and applications of photometry to practical problems in solar system exploration by spacecraft.

Eric M. De Jong is Chief Scientist for JPL's Instrument Software and Science Data Systems Section; and Research Director for JPL's: Visualization and Image Processing (VIP) Center, Image Processing Laboratory (IPL), Digital Image Animation Laboratory (DIAL), and Cartographic Analysis Laboratory (CAL). Eric is a Planetary Scientist in NASA's Jet Propulsion Laboratory Science Division and a Visiting Associate in Planetary Science at Caltech. For the last three decades his research has focused on the scientific visualization of the Earth; Sun; planetary surfaces, atmospheres, magnetospheres; and the evolution and dynamics of stars, galaxies and planetary systems. As the Principal Investigator for NASA's Space and Earth Science Visualization (SSV) Project he leads a team of scientists and technologists responsible for developing new science visualization products, infrastructure, technology, tools and services. De Jong and his team create movies, images, mosaics, maps and models from NASA Space & Earth Science remotely sensed data. These products highlight discoveries, science results, mission plans and operations. He received his B.S. in Plasma Physics from the Massachusetts Institute of Technology in 1967; M.S. in Plasma Physics from Stanford University in 1967, Ph.D. in Interdisciplinary Science from The University of California, Santa Barbara in 1982, and served as a Post-Doc in Planetary Science at Caltech in 1989.

Adnan Ansar received a BA (1993) in Physics, MA (1993) in Mathematics, MS (1998) in Computer Science and PhD (2001) in Computer Science all from the University of Pennsylvania, with the last earned at the GRASP Laboratory. He has been a member of the Robotics Section at NASA's Jet Propulsion Laboratory (JPL) since January, 2002. While at JPL, his research has included work on image based position estimation, camera calibration, stereo vision and multi-modal data registration.

Ted Scambos is a glaciologist and Lead Scientist at the National Snow and Ice Data Center at the University of Colorado, Boulder. He is a member of the Landsat Science Team, and a principal investigator on the Larsen Ice Shelf System, Antarctica (LARISSA) project for NSF, and numerous NASA grants investigating applications of remote sensing data to problems in polar and glacier mapping and climate change. Scambos received a B.S. in Earth and Space Sciences from the State University of New York at Stony Brook in 1977, an M.S. in Geology from Virginia Tech University in 1980, and a Ph.D. in Geology (Geochemistry) from the University of Colorado, Boulder in 1991. Scambos has conducted research on 16 expeditions to Antarctica, and has developed several innovative applications of satellite data to glaciological research, such as feature tracking, photoclinometry of ice sheets, and image super-resolution for mapping subtle ice flow features.

Paul Morin is the Director of the Polar Geospatial Center at the University of Minnesota. He manages a team that tasks, processes and delivers commercial satellite imagery to NSF and NASA cryosphere researchers. He is the US representative for geospatial data to the Antarctic treaty system. He is co-investigator on the Rapid Ice Sheet Change Observatory, a facility that aggregates data from 18 instruments, 5 agencies from four countries together to monitor ice around the globe.

Bernard Hallet studies diverse processes that sustain glaciers and shape landscapes in mountainous and polar regions. His extensive work on glacial erosion ranges from detailed theoretical analyses of the mechanics of glacial abrasion to field studies of rates of erosion and sediment production in Alaska, Patagonia, the Antarctic Peninsula and the Himalaya. In these regions, he also studies the rich linkages between climate, tectonics, and topography, and the response of glaciers to the changing climate.

Lonnie Thompson is recipient of the National Medal of Science; the Tyler Prize (the World Prize for Environmental Achievement); the International Science and Technology Cooperation Award of the People's Republic of China; and numerous other awards for his work on ice core paleoclimatology and global climate change. Thompson, a member of the National Academy of Sciences, was the first scientist to retrieve ice samples from a remote tropical ice cap.

Alex S. Gardner is an Assistant Professor at Clark University in the Graduate School of Geography. His research focuses primarily on the measurement and modeling glacier response to natural and human induced forcing and its impacts on sea level rise and water resources. He is a contributing author to two chapters of the Intergovernmental Panel on Climate Change's Fifth Assessment Report. Alex received a B.Eng. in Civil Engineering from the University of Saskatchewan in 2005 and a Ph.D. in Earth Sciences from the University of Alberta in 2010. He was a NSERC research fellow in the Department of Atmospheric, Oceanic, and Space Sciences at the University of Michigan between 2010 and 2012.

Jared Ekholm is a research scientist and Chief of the Cyber Integration and Transition Branch at the Air Force Research Laboratory, Information Directorate, Rome, NY . He serves as a research scientist in imaging science, hyperspectral imaging, and 3-D reconstruction and served as the lead technologist for several deployed intelligence collection systems. He received a B.S. in Physics from the University of Washington in 2003 and M.S. in Applied Physics from the Air Force Institute of Technology in 2012.